2 PIPPARD, A. B., BURRELL, O. J., and CROMIE, E. E.: 'The influence of re-radiation on measurements of the power gain of an aerial', *J. IEE*, 1946, **93**, Pt. 3A, pp. 720–722
3 BARLOW, H. M., and CULLEN, A. L.: 'Microwave measurements' (Constable, London, 1950)

METALLIC *E*-PLANE FILTER WITH CAVITIES OF DIFFERENT CUTOFF FREQUENCY

Indexing terms: Filters, Waveguides

A planar integrated circuit filter with multiple all-metal inserts and multiple abrupt waveguide step-wall discontinuities is introduced which achieves broadband high attenuation in the second stopband. The design is based on field expansion into suitably normalised eigenmodes which yield directly the modal *S*-matrix. This theory allows the immediate inclusion of both the higher-order mode interaction at all discontinuities and the finite thickness of the inserts. Computer-optimised design data for a five-resonator Ka-band prototype filter at 27 GHz midband frequency provide a minimum stopband attenuation of 50 dB between 27·5 and 44·5 GHz.

Introduction: All-metal inserts mounted in the *E*-plane of rectangular waveguides achieve low-cost low-insertion-loss filters[1–3] which have found widespread applications in channelisers, diplexers and mixers.[4] Common designs are composed of uniform halfwave resonator sections inductively coupled by single inserts,[1–3] or multiple parallel layers.[5,6] Extremely high rejection requirements over a broad second stopband, however, are difficult to meet by this kind of homogeneous filter if the passband is near the lower band limit of the corresponding waveguide mount. Since this behaviour depends on the relation between frequency and guide wavelength, to alleviate the problem the individual fundamental-mode cutoff frequency of each resonator may be suitably modified, for example by a gradual change of the corresponding waveguide width.

In this letter, therefore, an *E*-plane filter with cavities of different cutoff frequencies (Fig. 1) is investigated. The inductive junction effect of the step-wall discontinuities is utilised as an additional design parameter. Moreover, the coupling sections with a variable number of inserts require only thin strips of constant thickness which are well appropriate for low-cost production by photoetching techniques.

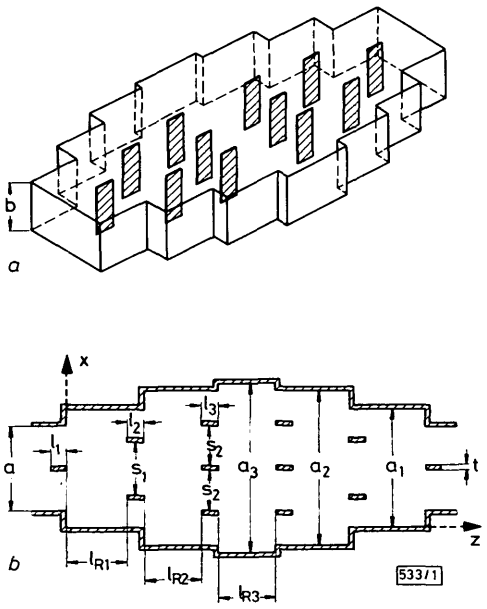

Fig. 1 *Metallic E-plane filter with unequal cavities*
a General view
b Dimensions of filter
l_i = strip length, t = strip width, a_i = cavity width, l_{Ri} = cavity (resonator) length, s_i = strip spacing, and a, b = initial waveguide dimensions

Theory and design: As in References 1–3, 5 and 6, the design of optimised filters is based on a rigorous field expansion technique into incident and scattered waves at all discontinuities. This allows direct inclusion of higher-order mode coupling, finite strip thickness and the step-wall discontinuity effects in the optimisation process.

For each corresponding subregion of the filter structure investigated (Fig. 1*b*), the fields

$$\vec{E} = -j\omega\mu\nabla \times \vec{\Pi}_{hx} \qquad \vec{H} = \nabla \times \nabla \times \vec{\Pi}_{hx} \tag{1}$$

are derived from the x-component of the magnetic Hertzian vector potential $\vec{\Pi}_h$, which is assumed to be a sum of suitably normalised eigenmodes satisfying the wave equation and the boundary conditions at the metallic surfaces:

$$\Pi_{hx} = \sum_{m=1}^{M} A_m^{\pm} T_m \sin\left(\frac{m\pi}{p} f\right) \exp\left(\pm jk_{zm} z\right) \tag{2}$$

where M is the number of eigenmodes considered, T_m is the normalisation factor so that the power carried by a given wave is 1 W for a wave amplitude of $1\sqrt{W}$, p is the cross-section dimension, f is the variable in the x-direction of the subregion considered,[1–3,5,6] and $k_{zm}^2 = k^2 - (m\pi/p)^2$, $k^2 = \omega^2\mu\varepsilon$.

By matching the tangential field components at the step discontinuity interfaces, the coefficients A_m in eqn. 2 are determined after multiplication with the appropriate orthogonal function. This leads directly to the two key building block scattering matrices necessary for this filter type, the scattering matrix of the n-furcated waveguide of finite length, and of the step-wall discontinuity of the change in width. The overall scattering matrix of the total filter is calculated without introducing transmission matrices by directly combining the single scattering matrices, which preserves numerical accuracy.

The computer-aided design is carried out by an optimising program,[2] applying the evolution strategy method, i.e. a modified direct search, where the parameters are varied statistically. For given initial waveguide housing dimensions, thickness, number and spacing of the inserts, and number and widths of resonators, the parameters to be optimised are the metal insert and resonator lengths, until the desired values of the insertion loss and of the stopband attenuation, for given bandwidths, are obtained. For computer optimisation, the expansion in 15 eigenmodes at each discontinuity has turned out to be sufficient. The final design data are checked by 45 eigenmodes.

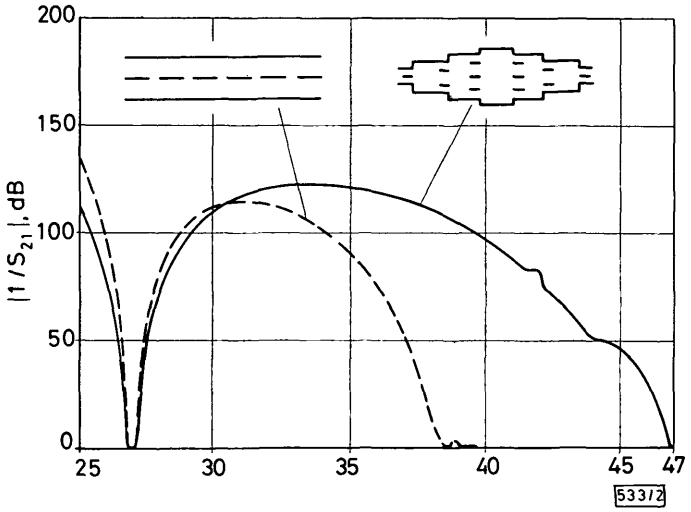

Fig. 2 *Insertion loss in decibels as a function of frequency of computer-optimised five-resonator E-plane filters*
Initial waveguide dimensions: a = 7·112 mm, b = 3·556 mm; thickness of all-metal inserts t = 0·19 mm
——— filter with multiple inserts and unequal cavities
Dimensions (cf. Fig. 1*b*): l_1 = 0·748 mm, l_2 = 2·349 mm, l_3 = 2·644 mm; l_{R1} = 5·843 mm, l_{R2} = 5·433 mm, l_{R3} = 5·122 mm; s_1 = 2·75 mm, s_2 = 2·50 mm; a_1 = 8·636 mm, a_2 = 10·668 mm, a_3 = 12·954 mm
– – – – – conventional *E*-plane filter (single insert, equal cavities)
l_1 = 0·76 mm, l_2 = 3·024 mm, l_3 = 3·201 mm; l_{R1} = 7·325 mm, l_{R2} = 7·396 mm, l_{R3} = 7·404 mm

Results: A five-resonator Ka-band filter is chosen for the design example (Fig. 2). For comparison, Fig. 2 shows the calculated insertion loss $1/|S_{21}|$ in decibels for a conventional metal insert filter (broken line), and for the filter with cavities of different waveguide widths (solid line). The advantage of the filter with inhomogeneous resonator sections is evident.

Conclusion: Broadband high attenuation in the second stopband is achieved by metallic *E*-plane filters with resonator sections of unequal waveguide widths. Moreover, the coupling sections are composed of a variable number of metal inserts which require only thin strips of constant thickness well appropriate for low-cost production by photoetching techniques. Since the computer-aided design is based on rigorous field expansion into eigenmodes, higher-order mode-coupling effects at all discontinuities and the finite thickness of the metal inserts are taken into account. The comparison with a conventional metal insert filter demonstrates the advantage of the filter type described with inhomogeneous resonator sections.

J. BORNEMANN
F. ARNDT

Microwave Department
University of Bremen
Kufsteiner Str., NW 1
D-2800 Bremen 33, W. Germany

4th March 1986

References

1 KONISHI, Y., and UENAKADA, K.: 'The design of a bandpass-filter with inductive strip—planar circuit mounted in waveguide', *IEEE Trans.*, 1974, **MTT-22**, pp. 869–873
2 VAHLDIECK, R., BORNEMANN, J., ARNDT, F., and GRAUERHOLZ, D.: 'Optimised waveguide *E*-plane metal insert filters for millimeter-wave applications', *ibid.*, 1983, **MTT-31**, pp. 65–69
3 SHIH, Y. C., and ITOH, T.: '*E*-plane filters with finite thickness septa', *ibid.*, 1983, **MTT-31**, pp. 1009–1013
4 MEIER, P. J.: 'Integrated fin-line: the second decade, Pt I', *Microwave J.*, 1985, **28**, pp. 31–54
5 ARNDT, F., BORNEMANN, J., VAHLDIECK, R., and GRAUERHOLZ, D.: '*E*-plane integrated circuit filters with improved stop-band attenuation', *IEEE Trans.*, 1984, **MTT-32**, pp. 1391–1394
6 BORNEMANN, J., and ARNDT, F.: 'Waveguide *E*-plane triple-insert filter'. Proc. of 15th European microwave conf., Paris, France, 1985, pp. 726–731

MAGNETOELASTIC AMORPHOUS METAL FLUXGATE MAGNETOMETER

Indexing terms: Magnetic devices, Magnetostrictive devices

A fluxgate magnetometer is presented which exploits the magnetic field dependence to the stress-driven magnetisation fluctuations in magnetostrictive metallic glass ribbons. A magnetometer constructed with an unannealed ribbon, a piezoelectric ceramic driving element and a 100-turn pick-up coil exhibits a minimum detectable magnetic field of 15 nT/$\sqrt{\text{Hz}}$ in the DC to 1 Hz bandwidth.

Amorphous metal ribbons and wires have been utilised in many sensor applications for the detection of a multitude of quantities including magnetic fields, stresses, displacement and current.[1] The detection of DC magnetic fields has been accomplished in two ways. These may be divided into the use of nonmagnetostrictive and magnetostrictive materials. Nonmagnetostrictive materials have been incorporated in a conventional fluxgate configuration and exhibit a minimum detectable field of 1·0 nT/$\sqrt{\text{Hz}}$.[2] Magnetostrictive materials have been mechanically interfaced to optical fibre interferometers which measure the field-induced strain in the ribbon. These devices currently exhibit a typical minimum detectable field of approximately 5·0 nT/$\sqrt{\text{Hz}}$.[3] Presented in this letter is the first amorphous metal fluxgate magnetometer which utilises the magnetoelastic response of a highly magnetostrictive ribbon. The intrinsic linearity of the magnetoelastic detection technique greatly simplifies the design, construction and electronic signal processing of the fluxgate magnetometer.

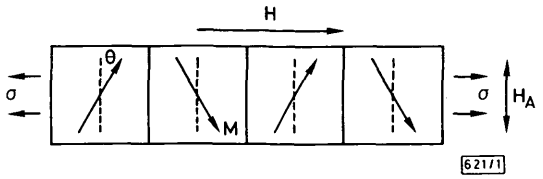

Fig. 1 *Field annealed amorphous metal ribbon exhibiting domain structure, anisotropy field H_A, applied field $\bar{H}$ and magnetisation M*

An amorphous metal ribbon which is annealed in the presence of a magnetic field directed along the width direction adopts a striped domain structure.[4] This is illustrated in Fig. 1. It is assumed that the response of the bulk field-annealed ribbon is adequately characterised by that of a single domain. The domain possesses a magnetisation vector of fixed magnitude M_D, which is confined to the plane of the ribbon, and is tipped by an angle θ with respect to the anisotropy axis characterised by the anistrophy field H_A.[5] A magnetisation M in the longitudinal direction results from the application of a longitudinal magnetic field H and stress σ. The material constitutive equation for the magnetisation is given by

$$M = \chi_0^\sigma H + \mu_0^{-1} d^H \sigma$$

where $\chi_0^\sigma = M_D/H_A$ is the magnetic susceptibility at constant stress, $d^H = 3\lambda_s \bar{H}/H_A^2$ is the piezomagnetic modulus at constant field, λ_s is the magnetostriction constant, and μ_0 is the permeability of free space.[6] $\bar{H}$ is the mean magnetic field and represents the low-frequency signal field. It is seen that an oscillating stress $\sigma(\omega)$ will induce magnetisation oscillations whose amplitude is proportional to the strength of the signal field. Magnetisation oscillations may be detected by a conventional pick-up coil. The electromotive force (EMF) ε generated in a pick-up coil of N turns is given by Faraday's law of induction: $\varepsilon = Nd\Phi/dt$, where $\Phi = BA$ is the magnetic flux, $B = \mu_0(M + H)$ is the magnetic induction, and A is the ribbon cross-sectional area. The EMF is found to be $\varepsilon(\omega_0) = NA\omega_0(3\lambda_s/H_A^2)\,\sigma_0 \bar{H} \cos \omega_0 t$, where a sinusoidal dependence is assumed for the stress oscillations of amplitude σ_0 and frequency ω_0. The magnetometer sensitivity η, defined as the change in EMF per unit of the signal field, is calculated to be $\eta = 3\lambda_s \omega_0 A(\sigma_0/\mu_0 H_A^2)$ V/T.

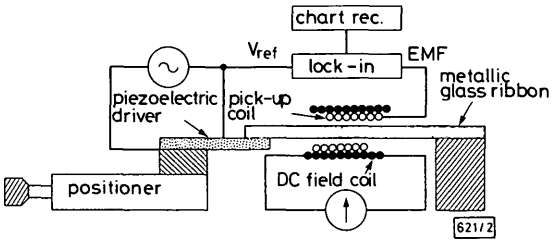

Fig. 2 *Magnetoelastic fluxgate magnetometer*

The viability of the proposed magnetic-field-sensing technique was tested experimentally. Fig. 2 illustrates the experimental apparatus. One end of an unannealed amorphous metal ribbon [Allied Corp. 2605S2, 30 μm thick, 0·5 in (12·7 mm) wide and 2 in (50·8 mm) long] was epoxied to the end of a piezoelectric plate. The free end of the ribbon was clamped to a stationary support structure. The piezoelectric plate was fastened to a second support structure mounted on a micropositioner. Movement of the micropositioner permits the adjustment of the equilibrium stress in the ribbon which optimises the magnetoelastic response. The central 0·5 in segment of the ribbon is surrounded by two coils. The first is the pick-up coil, consisting of 100 turns of copper wire. The second solenoid is a DC-field-producing coil of ~20 turns of 0·35 mm-diameter wire which is connected to a stable current source. The DC induction field produced by this coil is $B = \mu_0 nI$, where $n = 2{\cdot}9 \times 10^3$ m^{-1} is the number of turns per unit length and I is the current. The piezoelectric plate is driven by a voltage oscillator providing a 0·5 V amplitude voltage to the plate at a resonance frequency of ~100 kHz. The piezoelectric response of the plate drives the ribbon